The Influence of Counterion Structure Identity on Conductivity, Dynamical Correlations and Ion Transport Mechanisms in Polymerized Ionic Liquids

Zidan Zhang, Ram Krishna, Everett S Zofchak, Nico Marioni, Harnoor S Sachar, and Venkat Ganesan[a)]
McKetta Department of Chemical Engineering, University of Texas at Austin, Austin, Texas 78712, United States

(*Electronic mail: venkat@che.utexas.edu)

(Dated: 11 August 2023)

We used equilibrium and non-equilibrium atomistic simulations to probe the influence of anion chemistry on the true conductivity, dynamical correlations and ion transport mechanisms in PolyILs. An inverse correlation was found between anion self-diffusivities, ionic mobilities to the anion size for spherical anions. While some larger asymmetric anions had higher diffusivities than smaller spherical anions, their diffusivities and mobilities do not exhibit a direct correlation to the anion volumes. The conductivity and anion dynamical correlations also followed the same trends as displayed by the diffusivity and the mobility of anions. All the systems we examined displayed positively correlated motion among anions, suggesting a contribution which enhances the conductivity beyond the ideal, Nernst-Einstein value. Analysis of ion transport mechanisms demonstrated very similar hopping characteristics among the spherical anions despite differences in their sizes.

I. INTRODUCTION

Polymeric ionic liquids (PolyIL), which are macromolecules with one component of ionic liquids (IL) as repeat units (while the other ionic component remain as mobile counterions), have attracted increasing interest as electrolytes for energy storage materials.[1–5] PolyILs inherit the unique physicochemical properties from the corresponding IL, such as chemical stability and non-flammability,[6,7] while furnishing the ability to tune properties such as mechanical strength and conductivity.[8,9]

In the context of *monomeric* ILs, a number of experimental[10–12] and computational/theoretical[13–16] studies have probed the influence of chemical characteristics (size, symmetry, etc.) of the anion and cations on the dynamical properties of ILs. For instance, the diffusivity of ions were found to decrease with increasing size, reduced symmetry and decreasing flexibility of ions.[10,11,13,14] By investigating 29 ILs with different cation and anion structures, Maginn and coworkers found that the self-diffusivities and Nernst-Einstein conductivities exhibit universal linear relationship to the ion pair and ion-cage lifetimes.[17]

In contrast to the above situation, the understanding of the influence of anion/cation chemistry on the transport properties of PolyIL systems is relatively less developed.[18,19] In our recent study, we performed a comparative atomistic molecular dynamics simulation study of cationic polymerized ionic liquids with eight different mobile counterions, systematically varying size and shape of the anions to probe their influence on the coupling of the diffusivity to polymer segmental dynamics.[20] We demonstrated that size or ionic volume, couldn't fully rationalize the decoupling between anion diffusivity and the polymer segmental dynamics. However, within specified class of anion geometries, smaller ions generally displayed a higher degree of decoupling. Importantly, such size effects were observed not to be universal, but were modulated by the extent of delocalized interactions between the anions and the cations. In a different study, Paddison and coworkers investigated the ion transport mechanisms in polyILs for different anions.[16] They found that the dynamical heterogeneity in the motion of the ions decreased with the size of the anions. Further, they also noticed differences in the number of hopping events as a function of the chemistry of the anions.

An important feature characterizing many of the earlier computational studies on polyILs[21–24] is the implicit assumption that the self-diffusivity of the anion is representative of the conductivity of such materials. Such an expectation is based in turn on the validity of the Nernst-Einstein approximation for the conductivity. The latter assumes that the contributions arising from the correlated motion of distinct anions (and cations) can be neglected, and allows one to consider only the self-diffusivity of the anions in consideration of calculating conductivities.

Recent studies have however suggested that the above assumption may not hold for polyIL systems.[25,26] For instance, Wieland et al. demonstrated the importance of correlated ion motions in polyILs by reporting that the inverse Haven ratio (the ratio of true conductivity to the Nernst-Einstein approximation for conductivity) decreases monotonically with increasing degree of polymerization (N = 1, 2 and 3).[27] Correspondingly, in a recent atomistic simulation study, we demonstrated that the inverse Haven ratio increases with increasing degree of polymerization (N) and then decreases at larger N.[28] For a fixed center of mass reference frame, we demonstrated that such results arise as a consequence of the strong cation-cation correlated motions, which

---

[a)]https://sites.utexas.edu/ganesan/

exceed (in magnitude) the self-diffusivity of cations. Similarly, a number of experimental[29,30] or computational[31–33] studies in the context of monomeric ILs have also suggested the importance of such dynamical correlations (both between distinct anions/cations, and between the anions and cations) in influencing the overall conductivity of the material.

Motivated by the above recent findings, in the present study we revisited our earlier work on the role of counterion chemistry to focus on the true conductivity, and the dynamical correlations (the distinct anion-anion contributions) in polyIL systems and its relationship, if any, to the chemistry and geometry of the counterions.[20] Towards such an objective, we employ a non-equilibrium framework in conjunction with atomistic simulations to extract the true conductivity of polyIL materials.[24,28,34] Further, in combination with equilibrium simulations of the self-diffusivity of anions, we obtain the distinct dynamical correlations between anions. We also analyze in detail the dynamical characteristics accompanying the motion of the anions to identify the mechanisms of ion transport. Using such quantities we probe the influence of size and chemical features on the conductivity, dynamical correlations and the ion transport characteristics in such systems.

The rest of this paper is organized as follows: In section II, we present details of the the simulation details for equilibrium and non-equilibrium simulations, and the quantification measures. In section III, we discuss results for anion related dynamics (section III A), radial distribution functions (section III B) and ion hopping mechanisms (section III C). A brief summary is provided in section IV.

II. SIMULATION DETAILS

A. System Setup

Equilibrium simulation: Atomistic simulations were performed to probe the influence of anion structure (anion size and symmetry) on the conductivity and dynamical correlations in polyIL systems. The modeled polymer chain consists of fifteen 1-butyl-3-vinyl-imidazolium monomers, which has been extensively used in our previous studies.[20,21,23,35,36] To probe the effects of size and asymmetry of the anions (the detailed chemical structures are listed in FIG. 1), eight different anions were chosen: $AlCl_4^-$, BF_4^-, Br^-, Cl^-, PF_6^-, $PFSI^-$, $TFSI^-$and TFO^-. Among these, $AlCl_4^-$, BF_4^-, Br^-, Cl^-, PF_6^- are approximately spherical in shape, while $PFSI^-$, $TFSI^-$and $TFO^-$are non-spherical with delocalized partial charges.

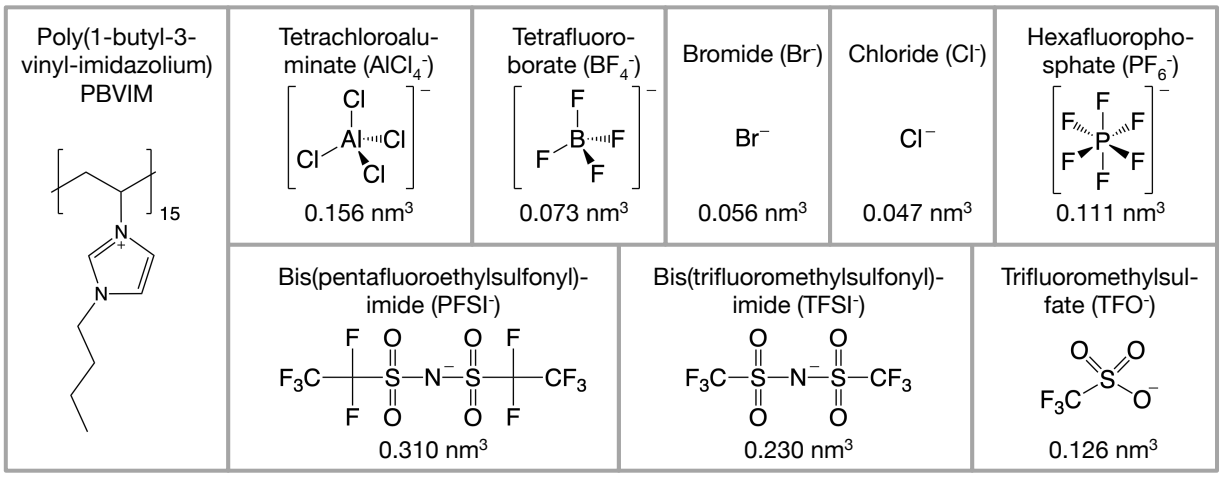

FIG. 1. Chemical details of the polyIL chain (PBVIM) and eight types of anions. The anionic volumes are obtained from refs.[37,38]

We used the all-atom optimized potential for liquid simulations (OPLS-AA) for describing the bonded and non-bonded interactions,[39] and the force field parameters for the polycation can be found in our previous work.[20] The partial charges for the polycation were adopted from another work of ours,[23] where the restrained electrostatic potential (RESP) charges are optimized over two trimers with different configurations. The partial charges for all investigated anions are adopted from Acevedo and coworkers' work.[40] Our recent work has demonstrated that using non-polarizable force field with scaled partial charges reproduces the structural and dynamical properties comparable to the polarizable force field.[41] Thus, a scale factor of 0.8 was applied to the charges on both polycation and anions.

For each of the simulation systems (polycation with counterions), twenty polymer chains (the degree of polymerization is 15), and 300 anions were inserted into a cubic box 8 nm long. Initially, these components were packed using Packmol.[42] A multistep pre-equilibration scheme was used to decompress the initial simulation box to its equilibrium density. Explicitly, each step consisted of three sub-steps: (i) 0.1 ns high temperature NVT simulation at 1000 K, (ii) 0.1 ns NPT simulation at desired

temperature (600 K) and high pressure (100 bar), and (iii), 0.1 ns NPT simulation at desired temperature and pressure (600 K and 1 bar).[43] In the present study, such a loop was repeated for 8 times.

The pre-equilibrated configuration that was obtained from the above decompression procedure was used for the production run with NPT ensemble for 420 ns, with the last 400 ns of the trajectory were used for analyzing the statistical and dynamical properties discussed below. Five independent samples with completely different initial configurations (replicates) were used for averaging the results. The time step Δt for the molecular dynamics was chosen as 1 fs. The v-rescale thermostat[44] and Parrinello-Rahman barostat[45] were used for temperature and pressure control, the corresponding coupling parameters τ_T and τ_P equal 1.0 ps, and the reference temperature and pressure were set to 600 K and 1 bar, respectively. The cut-off for the non-bonded interactions was 1.3 nm. Particle mesh Ewald method (PME)[46] was used to calculate electrostatic interactions.

Non-equilibrium simulations: The non-equilibrium simulations were executed with a series of external electric fields. We assume that all the investigated systems are isotropic, and hence the external electric field was only applied to the x-direction. The electric field strengths ranged from $0.02\ V/nm$ to $0.1\ V/nm$ with the increment of $0.02\ V/nm$. For the imidazolium-based polyIL systems, such a range of electric field strength has been demonstrated to guarantee a reliable linear response regime.[24,28] The final configuration that after 420 ns production run from the above equilibrium simulations was used as the input configuration for the non-equilibrium simulation. All the control parameters were the same as the equilibrium simulations, and a 40 ns production run was carried out for analyzing the ion displacements and extract the ionic mobility. Both the equilibrium and non-equilibrium simulations were performed using GROMACS 2020.6.[47]

B. Quantification Measures

Radial distribution functions: The structural characteristics of different functional groups were probed by calculating the radial distribution function $g(r)$ using Equation 1:

$$g_{ij}(r) = \frac{V}{4\pi r^2 N_i N_j} \left\langle \sum_i^{N_i} \sum_j^{N_j} \delta\left(r - r_{ij}\right) \right\rangle \tag{1}$$

where N_i and N_j are the number of particle species i and j of interests. V is the volume of simulation box, δ denotes the Kronecker delta function, and r represents the distance between the center of masses of units i and j. Further, the cut-offs for investigating the anion-polycation association characteristics in different systems were determined by the position r where $g(r) = 1.0$ after the first peak.

The non-Gaussian heterogeneity parameter α_2: The non-Gaussian heterogeneity parameter α_2 is an effective indicator of the dynamical heterogeneity in the motions of the units and the transition from the subdiffusive regime to the diffusive regime:

$$\alpha_2(t) = \frac{3\langle (r(t) - r(0))^4 \rangle}{5\langle (r(t) - r(0))^2 \rangle^2} - 1 \tag{2}$$

where $r(0)$ is the position vector of the given object at reference time, and $r(t)$ is the position vector of the given object at time t.

The self part of Van Hove function $G(r,t)$: The self part of Van Hove function $G(r,t)$ characterizes the distribution probability of a given anion travels a distance of r at time t, which can be calculated as:[48,49]

$$G(r,t) = \frac{1}{4\pi\rho N r^2} \sum_i^N \delta\left(r - |r_i(t) - r_i(0)|\right) \tag{3}$$

where ρ is the number density, N is the number of anions, δ is the Kronecker delta, $r(0)$ is the position vector of the given object at reference time, and $r(t)$ is the position vector of the given object at time t.

Self-Diffusivity (Diffusion coefficient): The self-diffusivity D of the anions were derived by fitting the mean-square displacement (MSD) to the following functional form:

$$\frac{\langle (\vec{r}(t) - \vec{r}(0))^2 \rangle}{6t} = D \cdot ((\frac{t}{t^*})^{-(1-\alpha)\gamma} + 1)^{1/\gamma}. \tag{4}$$

The above equation is proposed as a simple extrapolation between the short-time subdiffusive regime of the mean-square displacements (t^α, $\alpha < 1$) to its long-time diffusive regime. The parameter t^* denotes a crossover time between the subdiffusive and long-time diffusive regimes, and γ characterizes the shape of the crossover function.[50] $\vec{r}(t)$ is the position vector of the center of mass of anion at time t. The Fitted results and the corresponding details for all anions are shown in SI Section S1.1. In addition, the results from the traditional linear fitting[51] are shown in SI Section S1.2, and the comparisons between nonlinear and linear fitting are given in SI Section S1.3. From the results we can see that the fitted self-diffusion coefficients for anions are

comparable between the two methods, and the β values for the linear fits are all above 0.94 ($MSD \sim 6Dt^{\beta}$), demonstrating that the fitted anion self-diffusion coefficients are from the diffusive regimes.

Ionic mobility: Under each electric field strength, the drift velocity of the ions can be obtained from the linear regression of the displacement with respect to time t:

$$\langle v \rangle_- = \lim_{t\to\infty} \frac{1}{t} \langle \vec{r}_-(t) - \vec{r}_-(0) \rangle \tag{5}$$

Based on drift velocity results (SI Section S2), the first four points (five points in total) are used for fitting the ionic mobility through Equation 6:

$$\mu_- = \frac{\langle v \rangle_-}{E} \tag{6}$$

It has to be mentioned here that the reference frame used in the current study is polymer-centric reference frame, and thus, the total flux is fully accounted by the anionic mobility. We note that the magnitude of individual ionic mobility depends on the choice of reference frame, but however, the total flux and the true conductivities are independent of the reference frame.[28]

Conductivity: After obtaining the self-diffusion coefficients (from equilibrium simulations) and ionic mobilities (from non-equilibrium simulations), the ideal conductivity σ_-^{NE} and true conductivity σ_- can be calculated as:

$$\sigma_-^{NE} = \frac{\rho}{k_B T} z_-^2 D_- \tag{7a}$$

$$\sigma_- = F z_- c_- \mu_- \tag{7b}$$

where ρ is the number density of the total charge carriers, k_B is the Boltzmann constant, T is the temperature, z_- is the magnitude of the charge of anion, D_- denotes the self-diffusivities of anion, F is the Faraday's constant, c_- is the anion charge concentration, and μ_- is the anionic mobility. We note that under the polymer-centric reference frame (which has been suggested for polymer-based electrolytes[52]), μ_+=0, and the total true conductivity σ is identical to the anionic contribution σ_-. Recent studies have demonstrated that the self-diffusivity of the cation exhibits a scaling $D \sim N^{-2}$ with respect to the number of units of the polycation N. Hence, the cationic self-diffusivity contribution to the Nernst-Einstein conductivity is expected to be negligible relative to the anionic contribution.[53]

Distinct diffusivities and conductivities: The distinct (correlated) diffusion coefficients, D_{ij} ($i, j = -, +$), quantify the (average) influence of motion of ion of type i on ion j, and represents a measure of the non-ideal dynamical correlations in the system. We note that the choice of reference frame does influence the magnitude of dynamical correlations.[54,55] The distinct diffusion coefficients (D_{--} and D_{-+}) can be calculated from the self-diffusivity and the overall true conductivity σ (equals σ_- under polymer-centric reference frame)[24,28,33] with the following equations:

$$D_{--} = -\frac{D_-}{1-x_+} + \left(\frac{k_B T}{\rho e^2 (z_+ x_+)^2} \right) \sigma \tag{8}$$

$$D_{-+} = 0 \tag{9}$$

where x_+ and z_+ are the molar fraction and effective charge for cation, and ρ is the number density of the total charge carriers, k_B is the Boltzmann constant, T is the temperature. Further, the corresponding non-ideal contributions to the total conductivity, σ_{--}, can be obtained as:

$$\sigma_{--} = (\rho e^2 / k_B T)(1-x_+)^2 D_{--} \tag{10}$$

III. RESULTS AND DISCUSSION

A. Anion Related Dynamical Characteristics

Ion size has been suggested in a number of studies in the context of ILs and polyILs to be a critical parameter that influences the ion mobilities.[20] The anion size (in terms of the anionic volume[37,38]) for the ions chosen in this study are summarized in FIG. 2. The anions chosen in our study can be divided into two categories: the first five anions in FIG. 2 have a spherical shape with uniformly distributed partial charges, and the last three anions have a non-spherical shape with delocalized partial charges. It can be seen that the non-spherical anions have relatively larger size compared to the spherical anions.

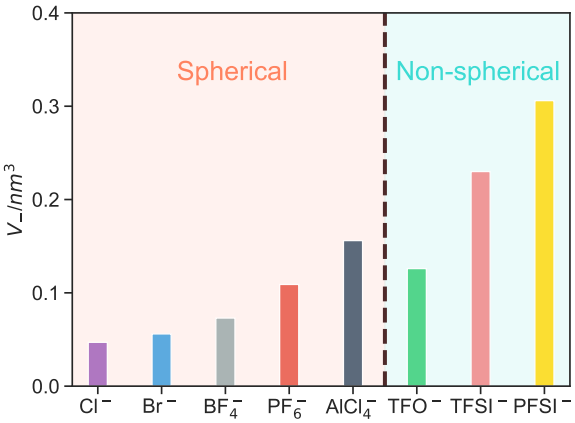

FIG. 2. Histogram showing the anion size (in volume) for all the anions in the current study.

As the first step to probe the influence of anion size on the ion transport properties in polyILs, we present the results of the diffusion coefficient and ionic mobility (FIG. 3) for different anions. The ionic mobilities of the anions that are displayed in FIG. 3(b) are seen to exhibit the same trends observed for the self-diffusion coefficients in FIG. 3(a). From FIG. 3(a) it can be seen that the anion $AlCl_4^-$ has the highest diffusivity, and the anion Cl^-has lowest diffusivity. Among the spherical anions, we observe an almost direct correlation between the anion size (volume) and its diffusivity, with the largest anion displaying the largest diffusivity. Anion pairs BF_4^- and PF_6^- represent outlier to such trends in which the diffusivity of BF_4^- is seen to be higher than PF_6^- despite its lower volume. More generally, the correlation between the diffusivity and the size is seen to break down when we include the asymmetric anions into consideration. Explicitly, larger anions such as $TFSI^-$and $PFSI^-$are seen to exhibit lower diffusivities compared to the more spherical $AlCl_4^-$ ion. Further, even among the asymmetric anions, the diffusivities are observed to be not correlated to the size of the anion, with $TFSI^-$possessing the highest diffusivity despite being intermediate in volume.

Next, we consider the behaviors of the total conductivity (obtained from the non-equilibrium simulations), the ideal Nernst-Einstein conductivity (obtained from the anion diffusivities, cf. Equation 7) and the dynamical correlations (in terms of distinct anion-anion diffusivity D_{--}, cf. Equation8) as a function of the counterion chemistry. In FIG. 3(c) we display the conductivities as a function of the different counterions examined in this work. It can be observed that the overall results exhibit the same trends observed for the anion diffusivities and mobilities. Explicitly, the conductivity (both the true and the Nernst-Einstein values) exhibits a direct correlation to the size for the spherical anions (excepting BF_4^- and PF_6^-). In contrast, among the asymmetric anions, we again observe that $TFSI^-$displays the largest magnitude of both total and ideal Nernst-Einstein conductivity despite being intermediate in size. Further, in comparison to spherical anions, we observe no clear correlation between the conductivities and the size in asymmetric anions.

Based on the true conductivities and the anion self-diffusivities (FIG. 3(a)), we can extract the dynamical correlations in terms of anion-anion distinct diffusivities D_{--}. The corresponding results are displayed in FIG. 3(d) for the different anions. Overall, the dependence of D_{--} on size of the anions is again seen to mirror the trends seen for the self-diffusivities and anionic mobilities. More interestingly, the distinct anion-anion diffusivities are seen to be positive and comparable in magnitude to the self-diffusivities of the anions. Such results (seen across the different counterions) suggest that the dynamical correlations cannot be neglected in consideration of the ionic conductivities of polyIL systems. Further, the positive sign of such correlations suggest that the anions exhibit correlated motion which enhances the overall conductivity of such systems (relative to the ideal Nernst-Einstein limit). The latter is consistent with the generally accepted notion of ion transport mechanism in polyILs which involves a process of hopping through a series of association-dissociation events involving coordination of the anion with different cations from more than one polymer chain.[21,23,35,36,49,56] Due to the ion-dense nature of polyIL systems, it can be expected that such hopping requires positively correlated motion of anions, as confirmed by the results of FIG. 3(d).

B. Cation-Anion Radial Distribution Functions

To understand the origins of the anion size dependency of the anion diffusivities and conductivities, we first turn to a consideration of the anion-cation radial distribution functions displayed in FIG. 4.[20,21,23,35,36,56] From the results displayed, we observe that, among the spherical anions, the intensity of the radial distribution functions mostly correlate inversely with the size of the anions. Such a trend also appears to hold when we observe that asymmetric ions, which in general possess larger volumes,

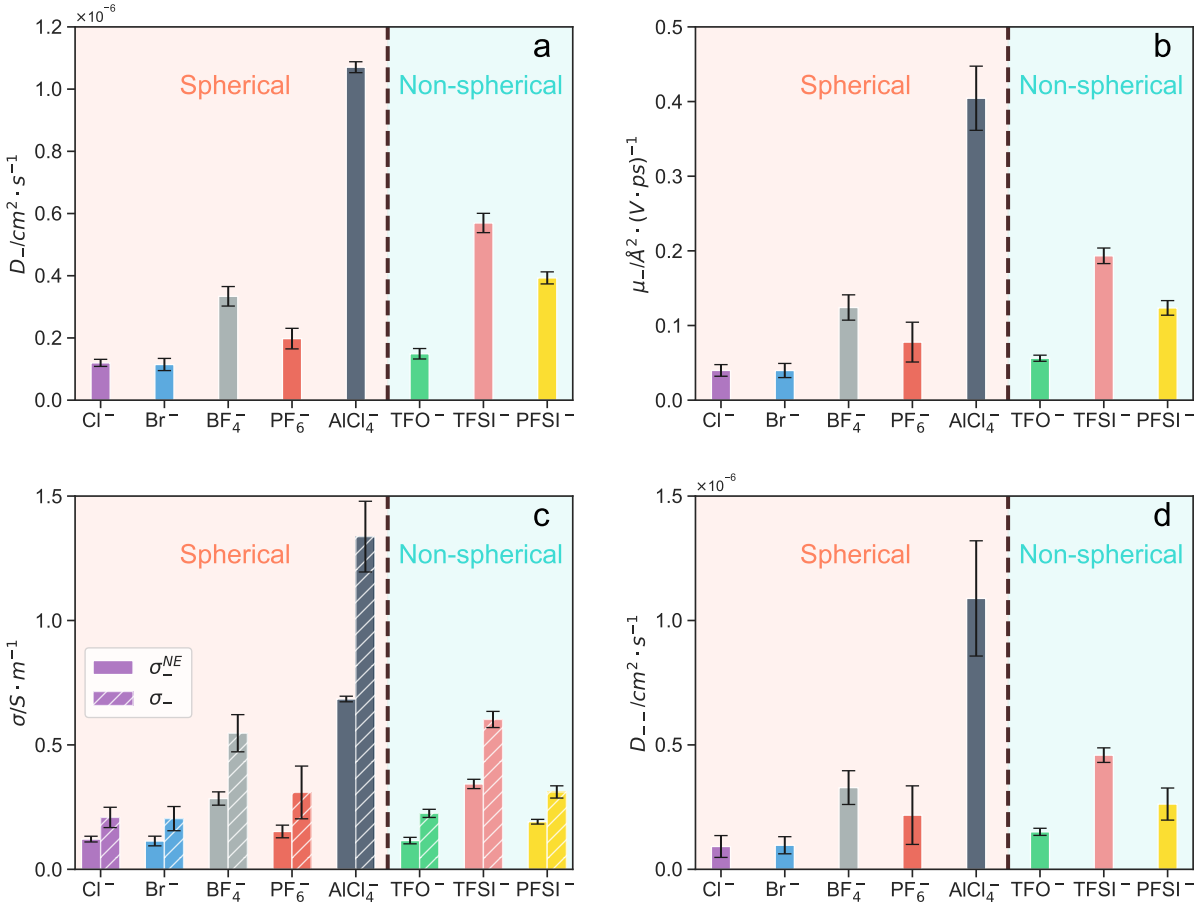

FIG. 3. (a) The self-diffusion coefficient for anion D_-, (b) the anionic mobility μ_- as a function of anion volume, the polymer-centric of mass was used as the reference frame, (c) The Nernst-Einstein σ_-^{NE} and true σ_- conductivities, and (d) the distinct anion-anion diffusivity D_{--}.

correspondingly exhibit weaker intensities of RDFs. Such results can be understood by noting that anion-cation interactions are primarily influenced by electrostatic interactions, which are inversely correlated to the size of the anions. However, we observe that at a quantitative level, size alone cannot explain the trends. For instance, we observe that $AlCl_4^-$ exhibits almost similar $g(r)$ characteristics as $TFSI^-$ and $PFSI^-$ despite possessing much smaller molecular volume. Similarly, PF_6^- exhibits higher intensity of $g(r)$ compared to BF_4^- despite its larger volume (size). Such results underscore the importance of the charge distribution (delocalization) on the anions in addition to size in determining the anion-cation interactions.

To understand the results observed for anion mobilities as a function of ion size, we note that there are two competing effects. On the one hand, smaller ions are expected to exhibit inherently greater mobility due to their size. Competing with such an effect is the stronger electrostatic interactions which accompany smaller ions, and seen in the RDF results displayed in FIG. 4. In comparing the RDFs with the diffusivity, mobility results of FIG. 3, we conclude that at least for the spherical anions, the slower mobility resulting stronger electrostatic interactions seems to dominate over the influence of size on mobilities. We observe that the intensity of the RDFs also explain the relative ordering of PF_6^- and BF_4^- diffusivities. However, in comparing the spherical ions to the asymmetric ions, the trends are a little less straightforward. We observe that TFO^- possesses the smallest size among the asymmetric anions and exhibits the strongest intensity of RDF. Consistent with the latter features, TFO^- exhibits the slowest diffusivity and mobility among the asymmetric anions. However, in comparing TFO^- with that of BF_4^-, we observe that BF_4^-, which possess a smaller volume and stronger anion-cation interactions (FIG. 4), exhibits a higher diffusivity. Such a result suggests that there is a competition between the delocalized electrostatic interactions resulting from larger sizes and the inherently higher mobilities of units possessing smaller sizes. Similar results are seen in comparing $PFSI^-$, $TFSI^-$ and $AlCl_4^-$ anions which exhibit comparable interaction characteristics, in which case the diffusivities seem to inversely correlate to their size. Together, such results demonstrate that both size and the extent of delocalization of charges (and the resulting electrostatic interactions) influence the anion diffusivities and the extent of anion-anion correlated motions.

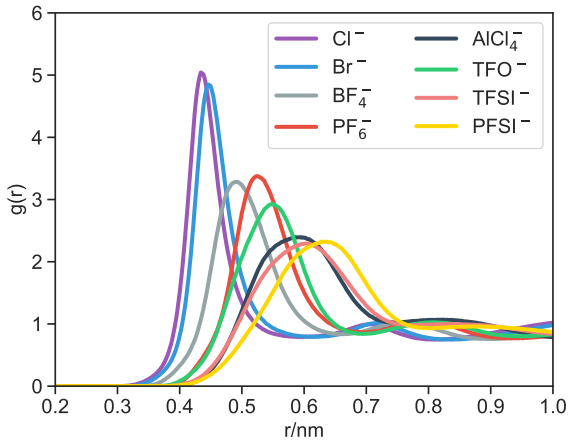

FIG. 4. The radial distribution function $g(r)$ for all investigated ions, both the cation (imidazolium ring) and the anions are adopting the center of mass.

C. Ion Transport Mechanisms

While consideration of RDFs provides a high level understanding of the observed diffusivity and mobility trends, it remains to be clarified whether there any inherent differences in the ions transport mechanisms which can be traced back to the physicochemical characteristics of the anion. As a background, we note that a number of past studies have established that anions in cationic polyILs are coordinated with multiple cations from distinct polymer chains.[20,21,35,36,49,56] The motion of such anions have been shown to involve a hopping like motion in which they "rattle" within their coordination shell for a certain period of time before executing a hop which refreshes one or more of their coordinating cations.[41,49] In this section, we quantify the different aspects accompanying such transport for the different anion chemistries.

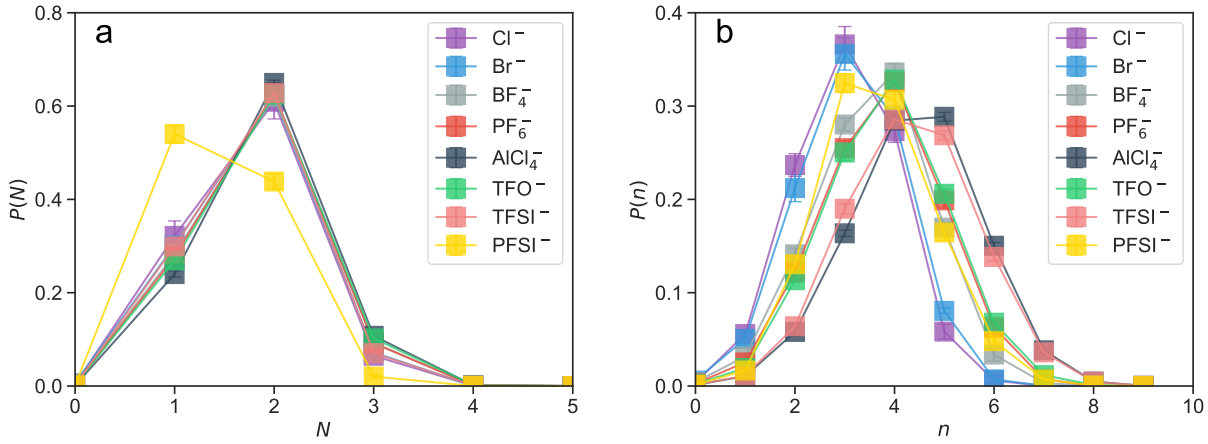

FIG. 5. (a) Probability that a given anion is associated with N polymer chains $P(N)$, (b) probability that a given anion is associated with n cations $P(n)$.

We start by characterizing the coordination characteristics (FIG. 5) of the different anions through the anion-polymer association function $P(N)$ (characterizing the probability that a given anion associates with N distinct polyIL chains) and the anion-cation association function $P(n)$ (characterizing the probability that a given anion associates with n distinct cations). From FIG. 5(a) we observe that for most of the investigated anions, regardless of the anion shape, a maximum of $P(N)$ can be observed at $N = 2$. The only exception is anion $PFSI^-$(the largest anion), for which a maximum of $P(N)$ can be observed at $N = 1$, but with still a broad peak with substantial probability for $N = 2$. In FIG. 5(b) it is seen that the peak of $P(n)$ can be found in the range of $n = 3$ to $n = 5$. Smaller anions ($Br^-$and Cl^-) are seen to prefer to associate with fewer cations ($n = 3$) and exhibit a narrower peak, while larger anions ($AlCl_4^-$ and $TFSI^-$) prefer to associate with more cations ($n = 4-5$) and exhibit a broader peak (again, the exception is found for anion $PFSI^-$, which prefers to associate with only three cations).

Overall, the above results demonstrate that despite significant differences in the physicochemical characteristics, the anions exhibit very similar coordination characteristics. As expected, asymmetric anions possessing more delocalized charges exhibit a broader distribution of coordination states compared to smaller, spherical anions.

In our recent paper,[41] we adopted the Paddison's method for characterizing anion hopping in polyILs. In brief, the methodology relies on a picture in which the anions "rattle" in its coordination shell for a period of time before executing a hop to its next coordination shell. The time scale of such hops is identified as the transition point from the subdiffusive regime to the diffusive regime in the motion of the anion, and can be obtained as the time at which the non-Gaussian heterogeneity parameter (Equation 2) $\alpha_2(t)$ attains a maximum.

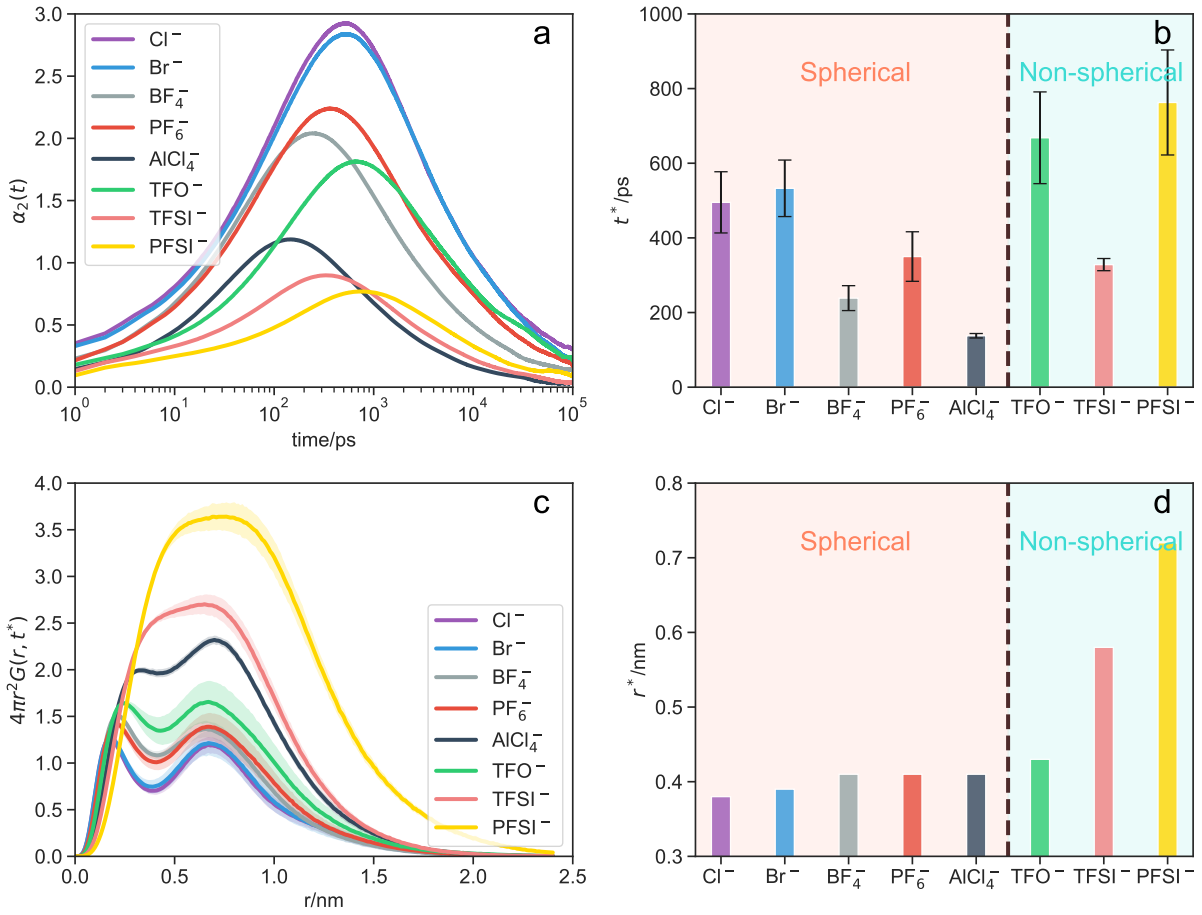

FIG. 6. (a) Non-Gaussian heterogeneity parameter $\alpha_2(t)$, (b) the temporal factor t^* at which the maximum of $\alpha_2(t)$ is located, (c) the self Van Hove function at t^*, and (d) the spatial factor r^* at where the first valley of $4\pi r^2 G(r,t^*)$ is located.

The results of $\alpha_2(t)$ for different anions are displaying in FIG. 6(a), where we can see that all α_2 profiles exhibit a single peak inside the time range from 100 to 1000 ps. Consistent with expectations, we observe that smaller ions, which possess stronger interactions with the cation, exhibit stronger dynamical heterogeneities in motion. The results for the corresponding time scale of hops, t^*, are shown in FIG. 6(b). Interestingly, the time scales t^* are seen to be (inversely) correlated to the size for the spherical anions (again, BF_4^- and PF_6^- constituting exceptions). However, in the case of asymmetric anions, the time scales for rattling (and the extent of dynamical heterogeneities) show no correlation to the size of the anion or to the intensity of the anion-cation interactions.

The next step in characterizing anion motion in polyILs, relies on identifying a spatial distance r^* which constitutes the distance to be traveled by the ions to be deemed to have executed a hop. With the obtained temporal factor t^*, the spatial factor r^* of different anions can be then evaluated by calculating the self part of Van Hove function $G(r,t^*)$ (cf. Equation 3), which characterizes the probability distribution that a given anion travels a distance of r at time t^*. FIG. 6(c) displays the results of self Van Hove function $G(r,t^*)$ for different anions, where we can see that the profiles of all the anions, except for $TFSI^-$and $PFSI^-$, exhibit exhibit two peaks. The outlier anions $TFSI^-$and $PFSI^-$are seen to instead exhibit a single broad peak. Generally, the first peak can be understood to correspond to the range of distance over which the anion is still rattling within its solvation shell. In contrast, the second peak can be understood to represent the transition (hopping) to the new position of the first solvation shell.

The position r^* at where the first valley of $G(r,t^*)$ is located is considered as the "distance" that a given anion must travel to execute an effective hopping event.

From the results displayed in FIG. 6, the self Van Hove functions $G(r,t^*)$ of $TFSI^-$ and $PFSI^-$ are seen to have only one broad peak, consistent with weaker dynamical heterogeneities seen in $\alpha_2(t)$ for such ions. Such results are also in agreement with those presented in Paddison's work which suggested that a single (and broad) peak may appear when the non-Gaussian heterogeneity parameter is weak (the intensity of $\alpha_2(t) < 1.5$).[49] In contrast, the intensity of dynamical heterogeneities in anion $AlCl_4^-$ is also smaller than 1.5, but relatively stronger than that of $TFSI^-$ and $PFSI^-$, and a double peak profile is observed. Since there is no valley observed in $G(r,t^*)$ for the $TFSI^-$ and $PFSI^-$ anions, we fit the profile by a sum of two single Gaussian functions (as shown in SI Section S3), to extract the spatial factor r^* for anions $TFSI^-$ and $PFSI^-$.

The spatial factor r^*s for different anions are shown in FIG. 6(d). Surprisingly, the r^* for those anions with spherical shapes are seen to be almost a constant around 0.4 nm, regardless of the size of the anion. In contrast, the r^* for those anions with non-spherical shapes differ significantly, with the r^* correlating with the size of the anion (i. e. $PFSI^- > TFSI^- > TFO^-$). Together, these results suggest that the spherical anions exhibit a rattling motion over a distance which is approximately independent of the size, but for a time which is correlated inversely to the size of the anions. In contrast, for asymmetric anions, the extent of rattling motion is much weaker (due to the delocalized interactions), and occurs over a larger length scale which correlates to the size of the anion.

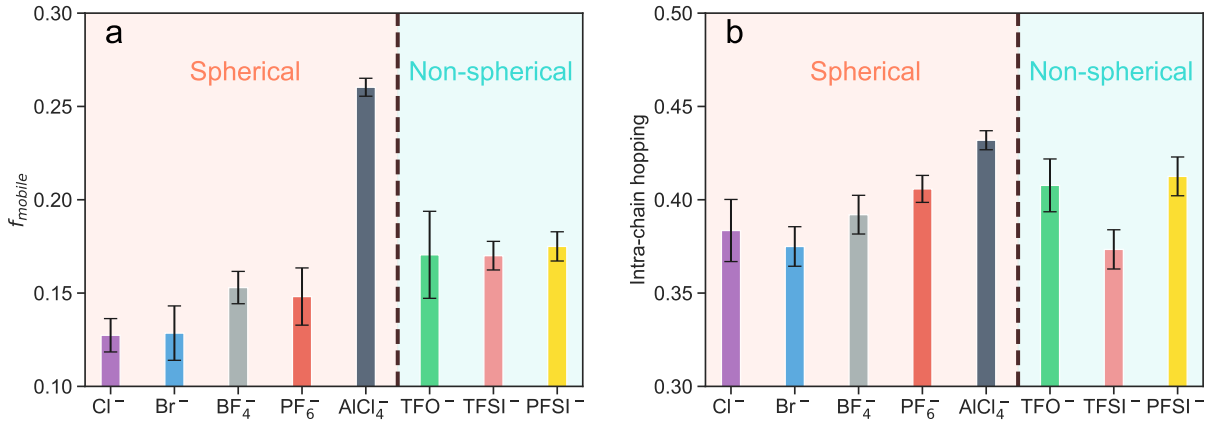

FIG. 7. (a) The fraction of mobile anions there are determined from both temporal and spatial scales (t^* and r^*), and (b) the fraction of intra-molecular hopping.

With the temporal and spatial factors identified for the different chemistries, mobile anions can be defined as those which travel at least a distance r^* within a given period t^* *and* whose one or more cations in the first solvation shell have changed their identities. The results for the fraction of such mobile anions are shown in FIG. 7(a). Therein, it can be seen that f_{mobile} is within a narrow range from 0.11 to 0.18, with an exception that f_{mobile} for $AlCl_4^-$ is about 0.26. Within the narrow range of values, the trends of f_{mobile} for anions with spherical shapes mirrors the size dependencies seen in diffusion coefficients and ionic mobilities. In contrast, the f_{mobile} for those anions with non-spherical shapes are seen to be almost independent of size and is approximately 0.17. Perhaps the more interesting result is the observation that despite significant differences in physicochemical characteristics and dynamical properties, the fraction of mobile ions is almost the same among the anions.

Upon identification of the mobile anions, we can identify the extent of intra and intermolecular hopping executed by the ions based on the identity of the cation which is refreshed in the solvation shell. The results for anion hopping analysis based on the mobile anions are shown in FIG. 7(b), wherein it can be seen that the fraction of intramolecular hopping is in a narrow range between 0.35 and 0.45. Such a result suggests that the intermolecular hopping has higher probability for all investigated anions regardless of their shapes and sizes. In addition, the size dependence of the fraction of intramolecular hopping of five anions with spherical shapes follows the trends seen for diffusion coefficient and ionic mobilities. In contrast, the dependence of the fraction of intramolecular hopping as a function of size for those anions with non-spherical shapes is seen to be opposite to the trends for diffusion coefficient and ionic mobility. Overall, it is seen that the anion physicochemical properties only exerts a minimal influence of the on the fraction of intra vs intermolecular hopping.

In summary, the results presented in this section illustrate several interesting characteristics of the mobile ion motion in polyILs and their dependencies on the anion chemistries. Overall, it was seen that the ions with larger sizes and/or delocalized charges exhibit weaker dynamical heterogeneities. Moreover, the timescale for hopping was seen to depend on the size of the anion for spherical ions, but was not correlated to the size for asymmetric ions. In contrast, among spherical anions, the distance required to execute a "hop" was not very sensitive to the size of ion, but for asymmetric ions, the distance required to execute a

hop was directly correlated to the size of the ion. Despite such differences, the fraction of mobile ions and the fraction of intra- and intermolecular hops were seen to be almost the same magnitude for all anions.

IV. CONCLUSIONS

In the present study, the influence of anion chemistry on the ion transport mechanism in PolyIL was probed by equilibrium and non-equilibrium atomistic simulations. An inverse correlation was found between anion mobility (self-diffusivity and ionic mobility) and anion size for spherical anions. While larger non-spherical anions had higher diffusivities than smaller spherical anions, their mobilities did not exhibit a clear correlation to the anion sizes. Both true and Nernst-Einstein conductivities, as well as the dynamical correlations, also followed the same trends as displayed by the diffusivity and the mobility anions. Surprisingly, all the systems we examined displayed correlated motion among anions, suggesting a positive contribution to the true conductivity. Analysis of ion transport mechanisms demonstrated very similar hopping characteristics among the anions despite significant different differences in their physicochemical features. Overall, our results confirm that ion transport in polyIL systems (containing a polycation) involve a complex interplay of size and charge delocalization characteristics.

ACKNOWLEDGEMENT

The authors work on the topic of ion transport in polymer electrolytes have been generously supported by grants from Robert A. Welch Foundation (Grant F1599), the National Science Foundation (DMR-2225167). The development of the non-equilibrium simulation methodology for ion conductivities was supported as part of the Center for Materials for Water and Energy Systems, an Energy Frontier Research Center funded by the U.S. Department of Energy, Office of Science, Basic Energy Sciences under Award #DE-SC0019272. The authors acknowledge the Texas Advanced Computing Center (TACC) for the generous allocation of computing resources. This material is based upon work supported by a National Science Foundation Graduate Research Fellowship under grant no. 000392968 to ESZ.

SUPPORTING INFORMATION AVAILABLE

Electronic supplementary information (SI) available: Section S1 is the nonlinear and linear fitting for the self-diffusion coefficient for both anions and cations, the comparison between the two is also presented; Section S2 is the fitting of the ionic mobility using non-equilibrium simulations, the polymer-centric reference frame was used; and Section S3 is the decomposition of the self Van Hove function for anions $PFSI^-$ and $TFSI^-$.

[1] W. Qian, J. Texter, and F. Yan, "Frontiers in poly(ionic liquid)s: syntheses and applications," Chem. Soc. Rev. **46**, 1124–1159 (2017).
[2] V. Ganesan, "Ion transport in polymeric ionic liquids: recent developments and open questions," Molecular Systems Design & Engineering **4**, 280–293 (2019).
[3] M. J. Park, "Confinement-entitled morphology and ion transport in ion-containing polymers," Molecular Systems Design & Engineering , 239–251 (2019).
[4] M. Forsyth, L. Porcarelli, X. Wang, N. Goujon, and D. Mecerreyes, "Innovative electrolytes based on ionic liquids and polymers for next-generation solid-state batteries," Accounts of Chemical Research **52**, 686–694 (2019), doi: 10.1021/acs.accounts.8b00566.
[5] V. Bocharova and A. P. Sokolov, "Perspectives for polymer electrolytes: A view from fundamentals of ionic conductivity," Macromolecules **53**, 4141–4157 (2020), doi: 10.1021/acs.macromol.9b02742.
[6] N. Nishimura and H. Ohno, "15th anniversary of polymerised ionic liquids," Polymer **55**, 3289–3297 (2014).
[7] G. G. Eshetu, D. Mecerreyes, M. Forsyth, H. Zhang, and M. Armand, "Polymeric ionic liquids for lithium-based rechargeable batteries," Molecular Systems Design & Engineering **4**, 294–309 (2019).
[8] N. Matsumi, K. Sugai, M. Miyake, and H. Ohno, "Polymerized Ionic Liquids via Hydroboration Polymerization as Single Ion Conductive Polymer Electrolytes," Macromolecules **39**, 6924–6927 (2006).
[9] D. Mecerreyes, "Polymeric ionic liquids: Broadening the properties and applications of polyelectrolytes," Progress in Polymer Science **36**, 1629–1648 (2011).
[10] S. Tsuzuki, W. Shinoda, H. Saito, M. Mikami, H. Tokuda, and M. Watanabe, "Molecular dynamics simulations of ionic liquids: Cation and anion dependence of self-diffusion coefficients of ions," The Journal of Physical Chemistry B **113**, 10641–10649 (2009), doi: 10.1021/jp811128b.
[11] S. Tsuzuki, H. Matsumoto, W. Shinoda, and M. Mikami, "Effects of conformational flexibility of alkyl chains of cations on diffusion of ions in ionic liquids," Physical Chemistry Chemical Physics **13**, 5987–5993 (2011).
[12] C. Iacob, A. Matsumoto, M. Brennan, H. Liu, S. J. Paddison, O. Urakawa, T. Inoue, J. Sangoro, and J. Runt, "Polymerized ionic liquids: Correlation of ionic conductivity with nanoscale morphology and counterion volume," ACS Macro Letters **6**, 941–946 (2017), doi: 10.1021/acsmacrolett.7b00335.
[13] M. H. Kowsari, S. Alavi, M. Ashrafizaadeh, and B. Najafi, "Molecular dynamics simulation of imidazolium-based ionic liquids. ii. transport coefficients," The Journal of Chemical Physics **130** (2009), 10.1063/1.3042279.
[14] H. V. Spohr and G. N. Patey, "Structural and dynamical properties of ionic liquids: Competing influences of molecular properties," The Journal of Chemical Physics **132** (2010), 10.1063/1.3380830.
[15] H. Liu and E. Maginn, "Effect of ion structure on conductivity in lithium-doped ionic liquid electrolytes: A molecular dynamics study," The Journal of Chemical Physics **139**, 114508 (2013), doi: 10.1063/1.4821155.
[16] X. Luo, H. Liu, and S. J. Paddison, "Molecular dynamics simulations of polymerized ionic liquids: Mechanism of ion transport with different anions," ACS Applied Polymer Materials **3**, 141–152 (2021).

[17] Y. Zhang and E. J. Maginn, "Direct correlation between ionic liquid transport properties and ion pair lifetimes: A molecular dynamics study," The Journal of Physical Chemistry Letters **6**, 700–705 (2015), doi: 10.1021/acs.jpclett.5b00003.
[18] M. Heres, T. Cosby, E. U. Mapesa, H. Liu, S. Berdzinski, V. Strehmel, M. Dadmun, S. J. Paddison, and J. Sangoro, "Ion transport in glassy polymerized ionic liquids: Unraveling the impact of the molecular structure," Macromolecules **52**, 88–95 (2019), doi: 10.1021/acs.macromol.8b01273.
[19] J. Li, R. He, H. Yuan, F. Fang, G. Zhou, and Z. Yang, "Molecular insights into the effect of asymmetric anions on lithium coordination and transport properties in salt-doped poly(ionic liquid) electrolytes," Macromolecules **55**, 6703–6715 (2022).
[20] J. R. Keith, N. J. Rebello, B. J. Cowen, and V. Ganesan, "Influence of counterion structure on conductivity of polymerized ionic liquids," ACS Macro Letters **8**, 387–392 (2019).
[21] S. Mogurampelly, J. R. Keith, and V. Ganesan, "Mechanisms underlying ion transport in polymerized ionic liquids," Journal of the American Chemical Society **139**, 9511–9514 (2017).
[22] E. W. Stacy, C. P. Gainaru, M. Gobet, Z. Wojnarowska, V. Bocharova, S. G. Greenbaum, and A. P. Sokolov, "Fundamental limitations of ionic conductivity in polymerized ionic liquids," Macromolecules **51**, 8637–8645 (2018), doi: 10.1021/acs.macromol.8b01221.
[23] Z. Zhang, J. Krajniak, J. R. Keith, and V. Ganesan, "Mechanisms of ion transport in block copolymeric polymerized ionic liquids," ACS Macro Letters **8**, 1096–1101 (2019).
[24] Z. Zhang, J. Sass, J. Krajniak, and V. Ganesan, "Ion correlations and partial ionicities in the lamellar phases of block copolymeric ionic liquids," ACS Macro Letters , 1265–1271 (2022).
[25] K. D. Fong, J. Self, B. D. McCloskey, and K. A. Persson, "Onsager transport coefficients and transference numbers in polyelectrolyte solutions and polymerized ionic liquids," Macromolecules **53**, 9503–9512 (2020).
[26] K. D. Fong, J. Self, B. D. McCloskey, and K. A. Persson, "Ion correlations and their impact on transport in polymer-based electrolytes," Macromolecules **54**, 2575–2591 (2021).
[27] F. Wieland, V. Bocharova, P. Münzner, W. Hiller, R. Sakrowski, C. Sternemann, R. Böhmer, A. P. Sokolov, and C. Gainaru, "Structure and dynamics of short-chain polymerized ionic liquids," The Journal of Chemical Physics **151**, 34903 (2019).
[28] Z. Zhang, B. K. Wheatle, J. Krajniak, J. R. Keith, and V. Ganesan, "Ion mobilities, transference numbers, and inverse haven ratios of polymeric ionic liquids," ACS Macro Letters **9**, 84–89 (2020).
[29] D. R. MacFarlane, M. Forsyth, E. I. Izgorodina, A. P. Abbott, G. Annat, and K. Fraser, "On the concept of ionicity in ionic liquids," Physical Chemistry Chemical Physics **11**, 4962–4967 (2009).
[30] K. Ueno, H. Tokuda, and M. Watanabe, "Ionicity in ionic liquids: correlation with ionic structure and physicochemical properties," Physical Chemistry Chemical Physics **12**, 1649–1658 (2010).
[31] M. Kunze, M. Montanino, G. B. Appetecchi, S. Jeong, M. Schönhoff, M. Winter, and S. Passerini, "Melting behavior and ionic conductivity in hydrophobic ionic liquids," The Journal of Physical Chemistry A **114**, 1776–1782 (2010), doi: 10.1021/jp9099418.
[32] K. R. Harris, "Relations between the fractional stokes-einstein and nernst-einstein equations and velocity correlation coefficients in ionic liquids and molten salts," The Journal of Physical Chemistry B **114**, 9572–9577 (2010), doi: 10.1021/jp102687r.
[33] H. K. Kashyap, H. V. R. Annapureddy, F. O. Raineri, and C. J. Margulis, "How Is Charge Transport Different in Ionic Liquids and Electrolyte Solutions?" The Journal of Physical Chemistry B **115**, 13212–13221 (2011).
[34] M. S. Alshammasi and F. A. Escobedo, "Correlation between ionic mobility and microstructure in block copolymers. a coarse-grained modeling study," Macromolecules **51**, 9213–9221 (2018), doi: 10.1021/acs.macromol.8b01488.
[35] J. R. Keith, S. Mogurampelly, F. Aldukhi, B. K. Wheatle, and V. Ganesan, "Influence of molecular weight on ion-transport properties of polymeric ionic liquids," Physical Chemistry Chemical Physics **19**, 29134–29145 (2017).
[36] Z. Zhang, J. Krajniak, and V. Ganesan, "A multiscale simulation study of influence of morphology on ion transport in block copolymeric ionic liquids," Macromolecules **54**, 4997–5010 (2021).
[37] H. D. B. Jenkins, H. K. Roobottom, J. Passmore, and L. Glasser, "Relationships among ionic lattice energies, molecular (formula unit) volumes, and thermochemical radii," Inorganic Chemistry **38**, 3609–3620 (1999), doi: 10.1021/ic9812961.
[38] W. Beichel, U. P. Preiss, S. P. Verevkin, T. Koslowski, and I. Krossing, "Empirical description and prediction of ionic liquids' properties with augmented volume-based thermodynamics," Journal of Molecular Liquids **192**, 3–8 (2014).
[39] W. L. Jorgensen, D. S. Maxwell, and J. Tirado-Rives, "Development and Testing of the OPLS All-Atom Force Field on Conformational Energetics and Properties of Organic Liquids," Journal of the American Chemical Society **118**, 11225–11236 (1996).
[40] B. Doherty, X. Zhong, S. Gathiaka, B. Li, and O. Acevedo, "Revisiting opls force field parameters for ionic liquid simulations," Journal of Chemical Theory and Computation **13**, 6131–6145 (2017).
[41] Z. Zhang, E. Zofchak, J. Krajniak, and V. Ganesan, "Influence of polarizability on the structure, dynamic characteristics, and ion-transport mechanisms in polymeric ionic liquids," The Journal of Physical Chemistry B **126**, 2583–2592 (2022).
[42] L. Martínez, R. Andrade, E. G. Birgin, and J. M. Martínez, "PACKMOL: A package for building initial configurations for molecular dynamics simulations," Journal of Computational Chemistry **30**, 2157–2164 (2009).
[43] G. S. Larsen, P. Lin, K. E. Hart, and C. M. Colina, "Molecular Simulations of PIM-1-like Polymers of Intrinsic Microporosity," Macromolecules **44**, 6944–6951 (2011).
[44] G. Bussi, D. Donadio, and M. Parrinello, "Canonical sampling through velocity rescaling," The Journal of Chemical Physics **126**, 14101 (2007), doi: 10.1063/1.2408420.
[45] M. Parrinello and A. Rahman, "Polymorphic transitions in single crystals: A new molecular dynamics method," Journal of Applied Physics **52**, 7182–7190 (1981).
[46] T. Darden, D. York, and L. Pedersen, "Particle mesh Ewald: An N·log(N) method for Ewald sums in large systems," The Journal of Chemical Physics **98**, 10089–10092 (1993).
[47] M. J. Abraham, T. Murtola, R. Schulz, S. Páll, J. C. Smith, B. Hess, and E. Lindahl, "Gromacs: High performance molecular simulations through multi-level parallelism from laptops to supercomputers," SoftwareX **1-2**, 19–25 (2015).
[48] Y. Shinohara, W. Dmowski, T. Iwashita, D. Ishikawa, A. Q. R. Baron, and T. Egami, "Local self-motion of water through the van hove function," Physical Review E **102**, 032604 (2020), pRE.
[49] H. Liu, X. Luo, A. P. Sokolov, and S. J. Paddison, "Quantitative evidence of mobile ion hopping in polymerized ionic liquids," The Journal of Physical Chemistry B **125**, 372–381 (2021).
[50] T. Ge, M. Rubinstein, and G. S. Grest, "Effects of tethered polymers on dynamics of nanoparticles in unentangled polymer melts," Macromolecules **53**, 6898–6906 (2020), doi: 10.1021/acs.macromol.9b01921.
[51] E. J. Maginn, R. A. Messerly, D. J. Carlson, D. R. Roe, and J. R. Elliot, "Best practices for computing transport properties 1. self-diffusivity and viscosity from equilibrium molecular dynamics [article v1.0]," Living Journal of Computational Molecular Science **1**, 6324–6324 (2019).

[52]C. Fang, X. Yu, S. Chakraborty, N. P. Balsara, and R. Wang, "Molecular origin of high cation transference in mixtures of poly(pentyl malonate) and lithium salt," ACS Macro Letters **12**, 612–618 (2023), doi: 10.1021/acsmacrolett.3c00041.
[53]P. Lan, Q. Zhao, G. Lv, G. S. Sheridan, D. G. Cahill, and C. M. Evans, "Molecular-weight dependence of center-of-mass chain diffusion in polymerized ionic liquid melts," Macromolecules (2023), 10.1021/acs.macromol.2c02388, doi: 10.1021/acs.macromol.2c02388.
[54]K. W. Gao, C. Fang, D. M. Halat, A. Mistry, J. Newman, and N. P. Balsara, "The transference number," ENERGY & ENVIRONMENTAL MATERIALS **5**, 366–369 (2022).
[55]Y. Shao, H. Gudla, D. Brandell, and C. Zhang, "Transference number in polymer electrolytes: Mind the reference-frame gap," Journal of the American Chemical Society **144**, 7583–7587 (2022).
[56]J. R. Keith and V. Ganesan, "Ion transport in backbone-embedded polymerized ionic liquids," The Journal of Chemical Physics **151**, 124902 (2019), doi: 10.1063/1.5121436.